SLAC-PUB-2982
September 1982
(T/E)

HEAVY QUARK FRAGMENTATION FROM e^+e^- ANNIHILATION AND νN SCATTERING EXPERIMENTS*

D. Schlatter
Stanford Linear Accelerator Center
Stanford University, Stanford, California 94305

1) Introduction.

The fragmentation of heavy quarks is both of theoretical and practical interest, but so far little is known about it. Most properties of the D meson have been determined within the first years of its discovery[1]. However, the fragmentation function of the D meson, or more generally that of charmed hadrons, has not been measured over a wide momentum range. At SPEAR energies the threshold was too high, D mesons could only be produced at the upper end of the spectrum[2]. Recently, several e^+e^- experiments have reported D^* production around 30 GeV[3-6]. There was already indirect evidence from measurements of the lepton spectrum in opposite side dilepton events in ν N scattering[7,8], indicating that charmed quarks fragment differently from light quarks. Substantially more neutrino scattering data is now available making it possible to extract a charm fragmentation function from $\mu^+\mu^-$ events[9]. Another neutrino experiment using emulsions[10] has observed several events with charmed hadrons and they have also measured the charm spectrum. Thus far, no one has been able to reconstruct a bottom meson and all new

* Work supported in part by the Department of Energy, contracts DE-AC03-76SF00515, W-7405-ENG-48, and DE-AC02-76ER03064.

(Talk presented at the 1982 SLAC Summer Institute on Particle Physics, Stanford, California, August 16-27, 1982.)

information on the bottom quark is indirect. Inclusive lepton spectra in e^+e^- annihilation allow one to determine semi-leptonic branching ratios[6,11-13] and the fragmentation function of the b-quark[14]. The heavy quark fragmentation functions, among other things, matter in understanding the inclusive hadron spectra and its energy dependence in e^+e^- annihilation. For a quantitative analysis and comparison to, e.g. QCD, one needs to know the heavy quark fragmentation functions.

2) Early Results.

In deep inelastic νN scattering charmed quarks are produced via the GIM mechanism[15]:

$$\nu + d\ (s) \rightarrow \mu^- + c$$

The second lepton, of opposite charge, originates from the semileptonic decay of the charmed particle:

$$c \rightarrow s + l^+ + \nu$$

The CDHS collaboration has were the first to study the charm fragmentation function[7] from this reaction. They observed about 315 $\mu^+\mu^-$ events in an exposure of the 200 GeV neutrino narrow band beam at CERN. The result of the normalized μ^+ spectrum is shown in fig. 1 as well as the expectations from different models. The only conclusion that could be drawn at the time was that charmed quarks fragment harder than light quarks.

The production of D-mesons in e^+e^- annihilation provides a particularly clean way to study the charmed quark fragmentation, since the initial quarks are "known" in this case. However, early measurements did not have enough energy in the center of mass to be well above the theshold for D production. The MARK I collaboration at SPEAR[2] could only observe D-mesons with $z=2E_D/E_{cm} > 0.6$ (the threshold is at $z=0.51$ at that energy). The result is shown in fig. 2.

Higher energy (for e^+e^-) and more statistics (for νN scattering) were needed to get better measurements.

3) Recent Results from νN Scattering Experiments.

In 1981 the CDHS collaboration has analysed 10380 $\mu^-\mu^+$ events in deep inelastic νN scattering[9] in the 400 GeV neutrino wide band beam at CERN. The large statistics allows the determination of the charm fragmentation function from a fit in bins of $z=E_D/E_c$ of the μ^+ spectrum, $z_\mu=p_\mu/(p_\mu+E_{hadron})$, and the hadron spectrum, $y_h=E_{hadron}/E_{tot}$. The result is shown in fig.3. The fragmentation function shows a peak around $z\simeq0.7$ with a very small contibuiton below 0.4. Since the data points are correlated the detailed shape cannot be obtained reliably. A simple delta function, $\delta(z-0.68)$, also gives an adequate fit to the data. However the average z is well determined and is $\langle z\rangle=0.68\pm0.08$ including systematic errors. Since the energy of the D meson is not measured in this experiment, a Monte Carlo model has been used to determine E_D. Also, one should remember, that this is a measure of the c quark fragmentation into any charmed hadron. D-mesons are only the dominant contribution.

A second neutrino scattering experiment, E531 at Fermilab, has used a different technique. The neutrino interaction took place in an emulsion and the outgoing particles were then measured in a downstream spectrometer[10]. A sketch of this experiment is shown in fig. 4a. All charm candidates were scanned and fully reconstructed. In a preliminary analysis ($\simeq$50% of their data) they obtained 42 charmed hadrons, unambiguously reconstructed. The resulting fragmentation function[16] is shown in fig. 4b, very similar to the one obtained by the CDHS group. Its average z value is $\langle z \rangle = 0.58 \pm 0.04$ (statistical error only).

4) Charm production in e^+e^- at high energies.

The observation of charmed mesons produced in high energy e^+e^- annihilation is more difficult compared with D production at SPEAR. The high multiplicity yields a large combinatorial background. Other means are necessary to reduce this background. In the reaction

$$D^* \rightarrow D\,\pi, \quad D \rightarrow K\pi$$

the kinematic constraint from the $D^* \rightarrow D$ decay with $\Delta M = 145$ MeV suppresses the background very efficiently. The first observation of D^*'s at high energies has been published by the MARK II collaboration at the PEP storage ring[3]. They have searched for the channels where the D^* is charged and the D is neutral. No positive particle identification has been used, the time-of-flight measurement was only required to be consistent with a pion or kaon assumption. Despite the good momentum resolution of $(\delta p/p)^2 = 0.015^2 + (0.006p)^2$ the combinatorial background does not allow one to observe the D-meson in the $K\pi$ spectrum. However, if the $K\pi$ mass is within ± 70 MeV of the D mass, a clear D^* signal is observed when fast $(z > 0.4)$ $D\pi$ candidates are selected (see fig. 5a). The corrected D^* spectrum is shown in fig. 5b for $z > 0.2$ (threshold is at 0.13 GeV). Again a similar shape as seen in the neutrino experiments is observed with an average $\langle z \rangle = 0.59 \pm 0.05$.

A second experiment at PEP, DELCO , has reported the observation of the D^* meson[5]. This detector is not particularly suited to reconstruct resonances in jet events. But the particular kinematics of the $D^* \rightarrow D\pi$

decay together with the particle identification capabilities of the DELCO detector make this analysis possible. The background in the spectrum of the mass difference $K\pi\pi$ - $K\pi$ is reduced considerably by kaon and pion identification thus compensating the poor mass resolution of 5 MeV. Fig. 6a shows a D^* peak above a small background, in particular for $z>0.4$. The fragmentation function is more flat than the ones obtained in the other experiments. Given the large errors at small z values there is good agreement with the MARK II result. One should also have in mind that the acceptance for D^* in the DELCO detector is rising from the threshold to its maximum in the second bin whereas it is constant for the MARK II detector for $z>0.2$

The largest sample of D^* events has been collected by the CLEO group[4] at the CESR storage ring at 10 GeV center of mass. They found 83 D^* events showing a clear signal in the $K\pi\pi$ - $K\pi$ mass difference (see fig. 7a). But the fragmentation function is only measured above $z>0.5$ (threshold is at 0.37). Therefore not much can be concluded about the shape of the fragmentation function. The TASSO group at PETRA has reported D^* production as well[6] but only for $z>0.5$. In Fig. 8 the mass differences of all 5 e^+e^- experiments are summarized.

5) Theoretical expectation.

Simple kinematical considerations[17] for a heavy quark fragmenting into a hadron containing Q (as sketched in fig. 9) lead to a different shape than the one from light quark fragmentation. The inertia of the heavy quark Q is retained by the $(Q\bar{q})$-meson, resulting in a harder fragmentation than if the quark masses can be neglected. Following these ideas and calculating the quantum mechanical transition probability for the process as shown in fig. 9 one gets the following fragmentation function[18]:

$$D_Q(z) = \frac{N}{z\ (\ 1 - 1/z - \epsilon_Q\ (1-z)\ )^2} \qquad (5.1)$$

where N is a normalization factor. The parameter ϵ_Q scales inversely with the square of the quark mass, $\propto 1/m_Q^2$. In fig. 10 this function is drawn for $\epsilon_Q = 0.25$ on top of the four measurements from νN and e^+e^- experiments. The agreement is remarkably good, given the systematically very different experiments and processes involved.

6) D^* Cross-section in e^+e^- Annihilation.

Besides the shape of the fragmentation function, the D^* cross section has been measured by several experiments. Two branching ratios ($B(D^*\to D)$ and $B(D\to K\pi)$) which are not measured very precisely enter into the total D^* cross section. The $D\to K\pi$ braching was taken to be (3±0.6)%[19] by all groups while there have been two values used for the $D^*\to D$ branching, (44±10)%[20] and (64±10)%[21]. In Fig. 11 the D^* cross section from all experiments has been plotted (assuming $B(D^*\to D)=64\%$). There is rather satisfactory agreement given the small data samples of each experiment. The total D^* cross section from MARK II, DELCO and CLEO are displayed in table 1. All results have a relatively large cross section (≃ 50% of the total $c\bar{c}$ production) but the error due to the branching ratios is big (≳ 25%).

Table I.

D^* cross section, $\sigma(D^{*+}+D^{*-})$ in nb, for two different values of $B(D^*\to D)$. The underlined values are the published ones.

Experiment	$B(D^*-D)=44\%$	$B(D^*-D)=64\%$	$c\bar{c}$	$b\bar{b}$
MARK II[22]	0.25±0.13	0.17±0.09	0.30	0.10
DELCO[5]		0.20±.06±.07	0.30	0.10
CLEO[4]	1.6±.04±.04	1.1±.03±.03	3.0	

7) Inclusive Electrons in Hadronic e^+e^- Events.

In the same way as the lepton spectrum from opposite-side dilepton events in deep inelastic neutrino scattering provides information on the charm fragmentation, the inclusive lepton spectrum in hadronic events in e^+e^- annihilation at high energies allows a determination of the charm and bottom fragmentation function. In particular at large transverse momentum of the lepton with respect to the jet axis, the bottom contribution becomes significant. Several experiments have used this signature to measure semileptonic branching ratios[6,11-14]. Table 2 summarizes these results.

Table II.

Semileptonic branching ratios (in %) from inclusive leptons in e^+e^-.

MARK J [11]	$B(c\to\mu)$ =	9.8±1.1±2.0
MARK II [14]	$B(c\to e)$ =	7 ± 2 ± 2
CUSB [12]	$B(b\to e)$ =	13.1±2.5±3.0
CLEO [13]	$B(b\to e)$ =	12.7±1.7±1.3
CLEO [13]	$B(b\to\mu)$ =	12.4±1.7±3.1
MARK J [11]	$B(b\to\mu)$ =	9.3±2.9±2.0
TASSO [6]	$B(b\to e)$ =	13.6±4.9±4.0
TASSO [6]	$B(b\to\mu)$ =	15.0±3.5±3.5
MARK II [14]	$B(b\to e)$ =	11.0±3.0±2.0

The Mark II collaboration has tried to determine the bottom fragmentation function simultaneously with the branching ratios since these quantities are correlated. This analysis selects electron candidates by requirement of a sufficient energy deposit (>50% of momentum) of a track in the first 8 radiation lengths of the liquid argon electromagnetic calorimeter. From 10691 e^+e^- hadron events in the MARK II detector at PEP, 1013 electron candidates were found, with substantial background. Misidentified hadrons give 425 events and there are 200 electrons from known sources other than charm and bottom. The data were plotted in bins of p and $p_\perp$ of the electron ($p_\perp$ with respect to the thrust axis) which are shown in fig. 12. A fit of a sum over 4 processes ($c \to e^-$, $b \to e^-$, $b \to c \to e^-$ and background) in four bins of z, the relative momentum in the fragmentation process, was performed. The charm fragmentation function was taken from the D* analysis (actually the formula 5.1 with $\epsilon_c=0.30$ was used). Since there were not enough data to determine several bins of the bottom fragmentation function, the same shape of equation 5.1, but ϵ_b as free parameter, was assumed. The result for the three parameters is $B(c \to e)=0.07 \pm 0.02 \pm 0.02$, $B(b \to e)=0.11 \pm 0.03 \pm 0.02$ and $\epsilon_b=0.04\ -0.025+0.035$ with a $\chi^2=13.6$ for 18 degrees of freedom. Data points were not used in the fit where the background is dominant ($p < 4$ GeV $- 2p_\perp$(GeV)). The fit result is a very good description of the data (see fig. 12) even in the area excluded from the fit. Fig. 13 shows the decomposition of the electron spectrum for two different $p_\perp$ intervals. There is a dominance of the electronic bottom decay fot $p_\perp > 1$GEV and $p > 3$ GeV.

The result of the bottom quark fragmentation function is displayed in fig. 14. It exhibits a much harder spectrum for bottom quarks than for charm quarks. For curiosity one can scale the parameter $\epsilon_c=0.3$ with m_c^2/m_b^2 and gets $\epsilon_b=0.03$ compared to the measured 0.04.

8) Inclusive Hadron Spectra and Scale Breaking in e^+e^- Annihilation.

The observation of scaling violations in the nucleon structure functions from deep inelastic lepton-nucleon scattering experiments has significantly supported the notion of QCD and gluon bremsstrahlung. Similar patterns of scale breaking are expected in the energy dependence of fragmentation functions[23]. Therefore much attention has been paid to the measurements of the inclusive charged particle cross section in hadronic events in e^+e^- interactions. The differential cross section, $sd\sigma/dx$ (or $1/\sigma d\sigma/dx$), with x the fractional energy of the particle, has been measured by several groups. The systematic limitations in comparing measurements from different detectors at different energies at first did not allow one to observe the scaling violation effects. Only when the same detector had measured $sd\sigma/dx$ at different energies[24] was the expected scale breaking pattern observed. Recently, there have been more measurements from different groups[25,26] in good agreement with each other in the energy interval of 5 GeV to 35 GeV. In Fig. 15 the quantity $1/\sigma d\sigma/dx$ is displayed for x>0.1 from the TASSO and MARK II experiments. The relative uncertainty between the two experiments is 10%. At large values of x a strong decrease of the cross section with energy is observed (a factor 2 from 5 GeV to 35 GeV). The same was found by the PLUTO group[6] (fig.16). One can use the following parameterisation for the energy dependence:

$$sd\sigma/dx = b\ (\ 1 + c_1 \ln s(\text{ GeV})\ )$$

The coefficient c_1, a measure of the strenght of the sacling violation, is given in fig. 17 in good agreement from all three experiments.

The interpretation of these results is however difficult[27]. In a purely perturbative frame of QCD, scaling violation emerges only from gluon bremsstrahlung off the quarks, and non-perturbative effects from masses and transverse momenta in the subsequent fragmentation into hadrons are ignored. Indeed, such a picture[28] is able to account for the observed scaling violations with a QCD parameter $\Lambda \simeq 200$ MeV[18]. The other extreme considers only the non-perturbative contributions. A Monte Carlo simulation[29] of the fragmentation of the u,d and s quark only, yields most of the observed scale breaking (dotted line in fig. 18). The addition of the heavy charm quark, with its different fragmentation function, as discussed above, seems to be important, in particular at high energies. Finally the radiation of a hard gluon brings this model in good agreement with the data[30] (see full line in fig. 18).

In conclusion deciphering fragmentation functions seems to be difficult. Mass effects and heavy quark fragmentation are important unless much higher energies are reached.

References and Footnotes.

1. G. Goldhaber et al., Phys.Rev.Lett. 37(1976) 255.

2. P. A. Rapidis et al., Phys.Lett.84B (1979) 507.

3. J.M. Yelton et al., Phys.Rev.Lett.49(1982),430

4. C. Bebek et al., Phys.Rev.Lett.49(1982) 610.

5. W.B. Atwood,SLAC-PUB 2980 (1982).

6. D. Lüke, Proc. XXI Intern. Conf. on High Energy Physics,Paris (1982).

7. M. Holder et al.,Phys.Lett.69B (1977) 377.

8. N. Armenise et al.,Phys.Lett.86B(1979)115.

9. H. Abramovicz et al., CERN-EP/82-77 (1982)

10. N. Ushida et al.,Phys.Rev.Lett.45(1980)1049.

11. J.D. Berger,Proc. XXI Intern. Conf. on High Energy Physics,Paris (1982).

12. L.J. Spencer et al.,Phys.Rev.Lett.47(1981) 771.

13. C. Bebek et al,Phys.Rev.Lett. 46(1981) 84,
K. Chadwick et al.,Phys.Rev.Lett. 46(1981) 88.
and K. Chadwick et al.,CLNS 82/546(1982) preprint.

14. G.H. Trilling,Proc. XXI Inter. Conf. on High Energy Physics,Paris (1982).

15. S. L. Glashow, J. Iliopoulos, L. Maiani, Phys.Rev. D2 (1970) 1285.

16. S.M. Errede,Rx-966(Ohio-State)1981,Ph.D.Thesis unpublished and private communication.

17. J. D. Bjorken, Phys.Rev.D17(1978) 171
and M. Suzuki, Phys.Lett.71B(1977) 189

18. C. Peterson et al. SLAC-PUB-2912 (1982).

19. G. J. Feldman et al.,Phys.Rev.Lett.38(1977) 1313.

20. M. W. Coles et al.,SLAC-PUB-2916 (1982).

21. G. Goldhaber et al.,Phys.Lett.69B(1977) 503.

22. This cross section is smaller than the published value[3] which was obtained from a smaller data sample.

23. J. Owens,Phys.Lett.76B(1978)85

T. Uematasu,Phys.Lett.79B(1978)97.

24. R. Hollebeek,Proc. 1981 Intern. Symposium on Lepton and Photon Interactions at High Energies, Bonn,p1.

25. R. Brandelik et al.,DESY 82-13 (1982).

26. J. Patrick et al.,SLAC-PUB-2936 (1982).

27. A detailed discussion can be found in ref. 18.

28. E.G. Floratos et al.,Nucl.Phys.B192(1981)417.

29. The LUND Monte Carlo program was used.

T. Sjostrand, LU TP 80-3 and LU tp 82-3.

30. In the comparison of fig. 18 the Monte Carlo parameters have been adjusted to the MARK II data. This may account for the poorer fit of the TASSO data.

Figure Captions.

1. Muon spectrum, $z=E_\mu/(E_\mu + E_{had})$, from early CDHS $\nu N \to \mu^-\mu^+ + h$ scattering.

2. D spectrum from MARK I at SPEAR.

3. Charm fragmentation from the CDHS νN experiment.

4. a) E531 ν-emulsion experiment at FNAL.

   b) Charm fragmentation from E531 ν-emulsion experiment.

5. D^* results from MARK II at PEP.

   a) $D^0\pi - D^0$ mass difference.

   b) D^* fragmentation function.

6. D^* results from DELCO at PEP.

   a) $D^0\pi - D^0$ mass difference.

   b) D^* fragmentation function.

7. D^* results from CLEO at CESR.

   a) $D^0\pi - D^0$ mass difference.

   b) D^* fragmentation function.

8. $D^0\pi - D^0$ mass difference from 4 different e^+e^- experiments.

9. The fragmentation of a heavy quark Q into a meson $(Q\bar{q})$.

10. Charm fragmentation function from νN and e^+e^- experiments. The curve is eq. 5.1 with $\epsilon_Q = 0.25$.

11. D^* cross section in e^+e^- with $B(D^* \to D)=0.64$ and $B(D \to K\pi)=0.03$.

12. Inclusive electron spectrum from MARK II for different transverse momentum. The full line is the result of a fit of $c \to e^-$, $b \to e^-$, $b \to c \to e^-$ and background. The hatched area was excluded in the fit.

13. Components of the electron spectrum from a fit to the MARK II data.

14. Heavy quark fragmentation functions, normalized to 1. The bottom

quark function is a fit result of equ. 5.1 to the MARK II data. The hatched area indicate the 1σ limits.

15. Inclusive hadron spectrum from TASSO and MARK II.

16. Inclusive hadron spectrum from PLUTO.

17. Strength of the scaling violations from TASSO and PLUTO, $s d\sigma/dx \propto 1 + C_1 \ln s(\text{GeV})$.

18. Ratio of $s d\sigma/dx$ at two different energies. The dotted line is a Monte Carlo simulation with u,d and s quarks only. The dashed lines include C quarks. The full line includes hard gluon emission. a) MARK II data. b) TASSO data.

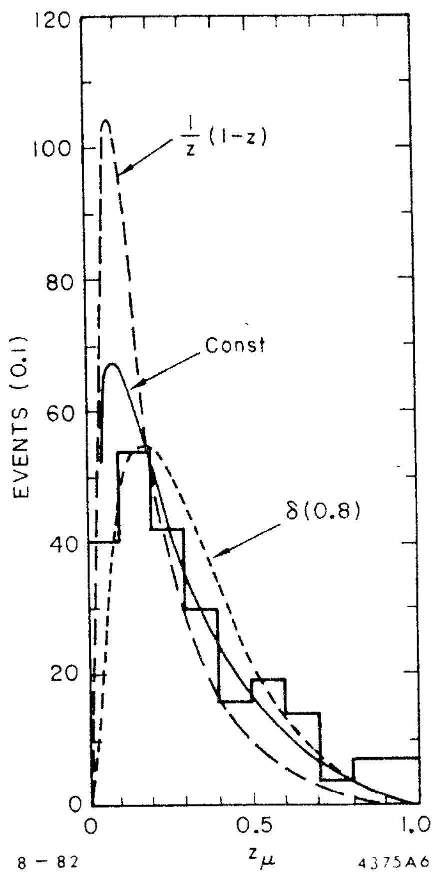

120
100
80
60
40
20
0
EVENTS (0.1)
$\frac{1}{z}$ (1-z)
Const
δ(0.8)
0
0.5
1.0
z_μ
8 - 82
4375A6

Fig. 1

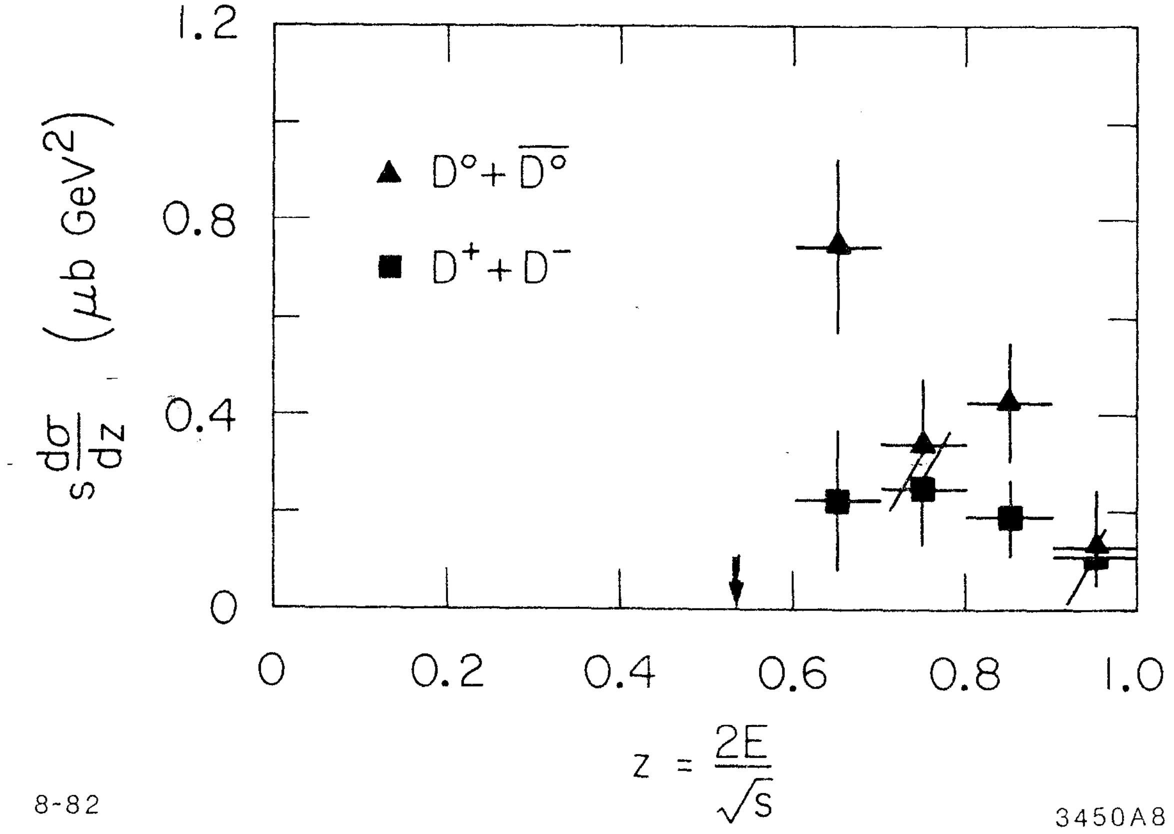

Fig. 2

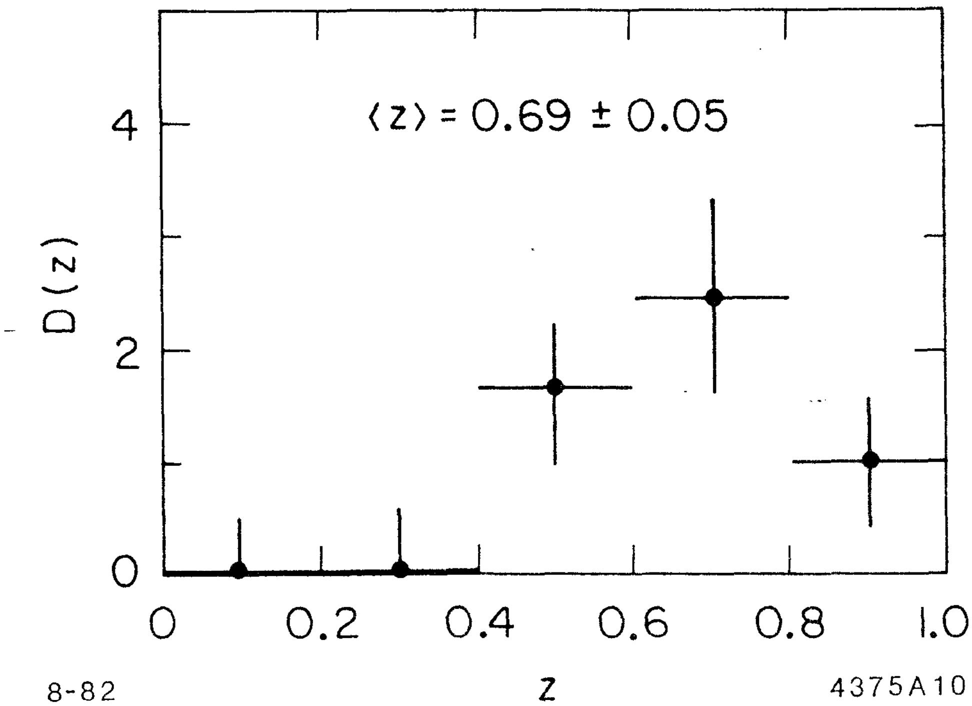

Fig. 3

Fig. 4a

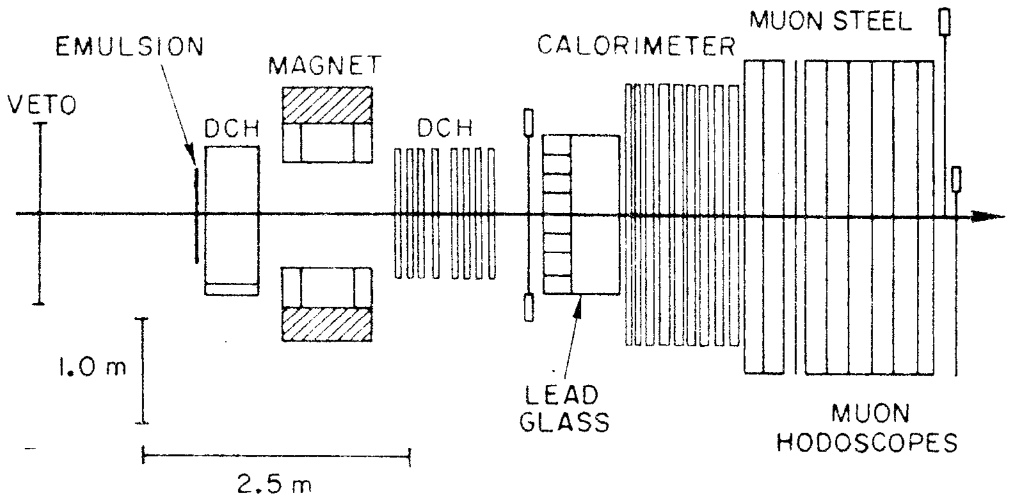

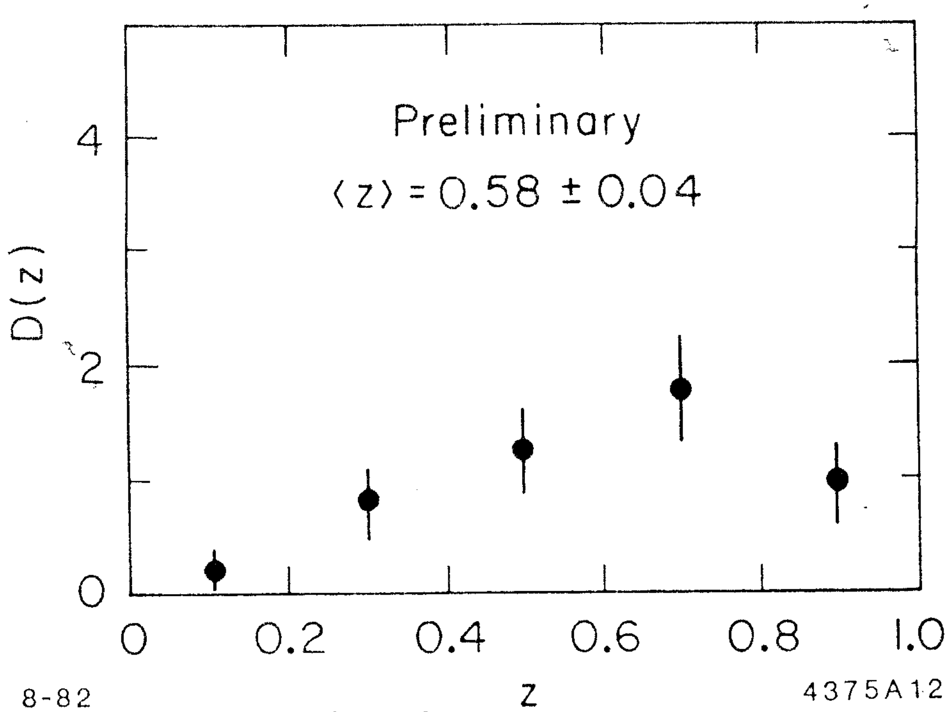

Fig. 4b

Fig. 4b

Fig. 5a

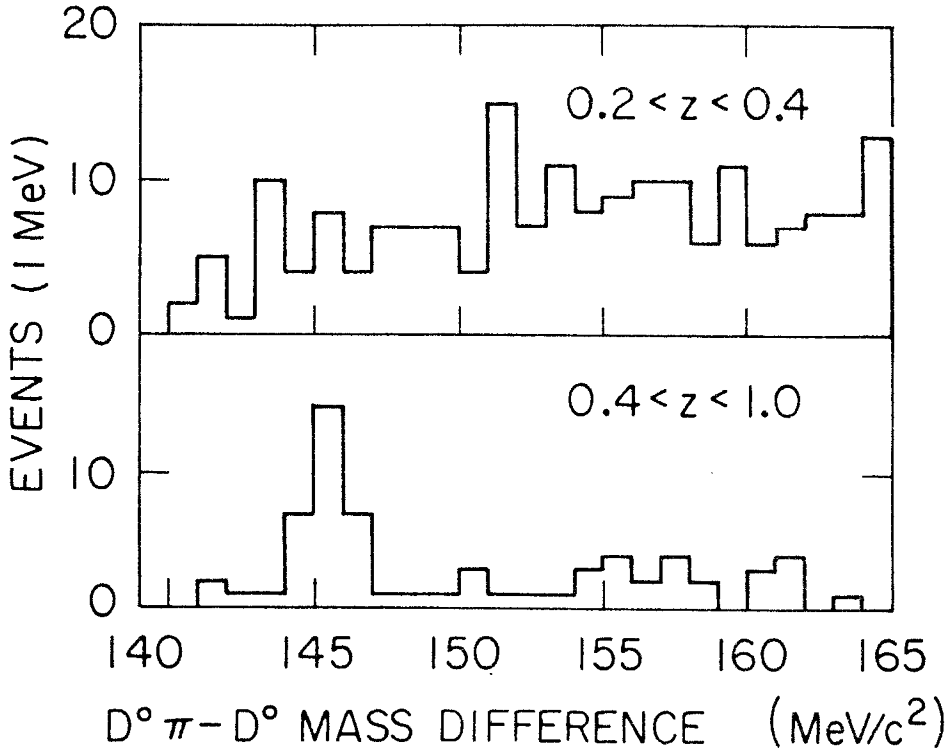

20
10
0
10
0
0.2 < z < 0.4
0.4 < z < 1.0
EVENTS (1 MeV)
140
145
150
155
160
165
D° π − D° MASS DIFFERENCE (MeV/c²)

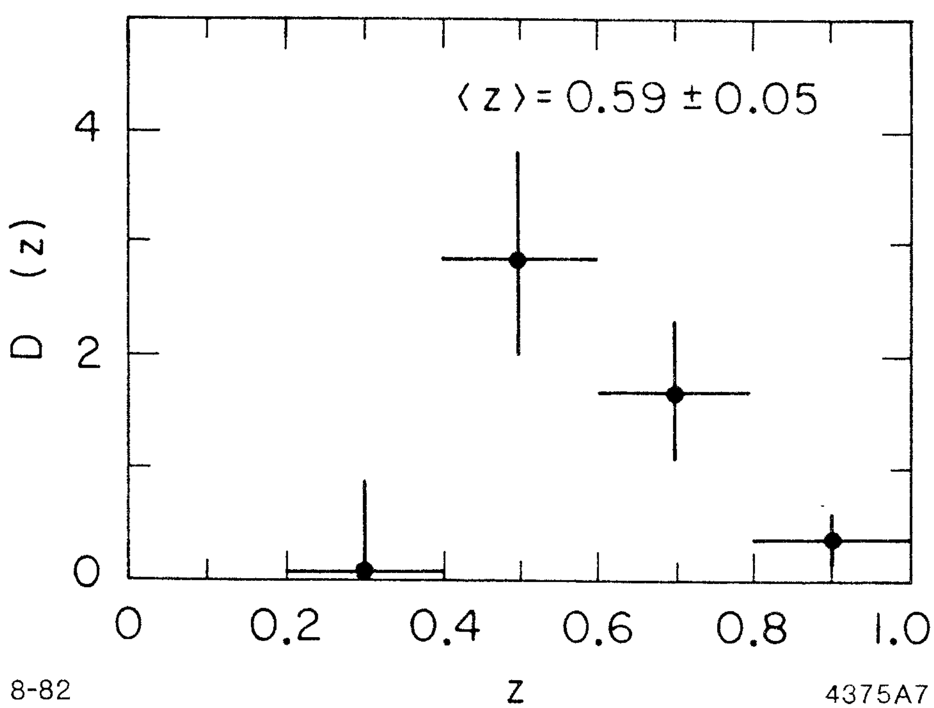

⟨z⟩ = 0.59 ± 0.05
4
2
0
D (z)
0
0.2
0.4
0.6
0.8
1.0
8-82
z
4375A7

Fig. 5b

Fig. 6a

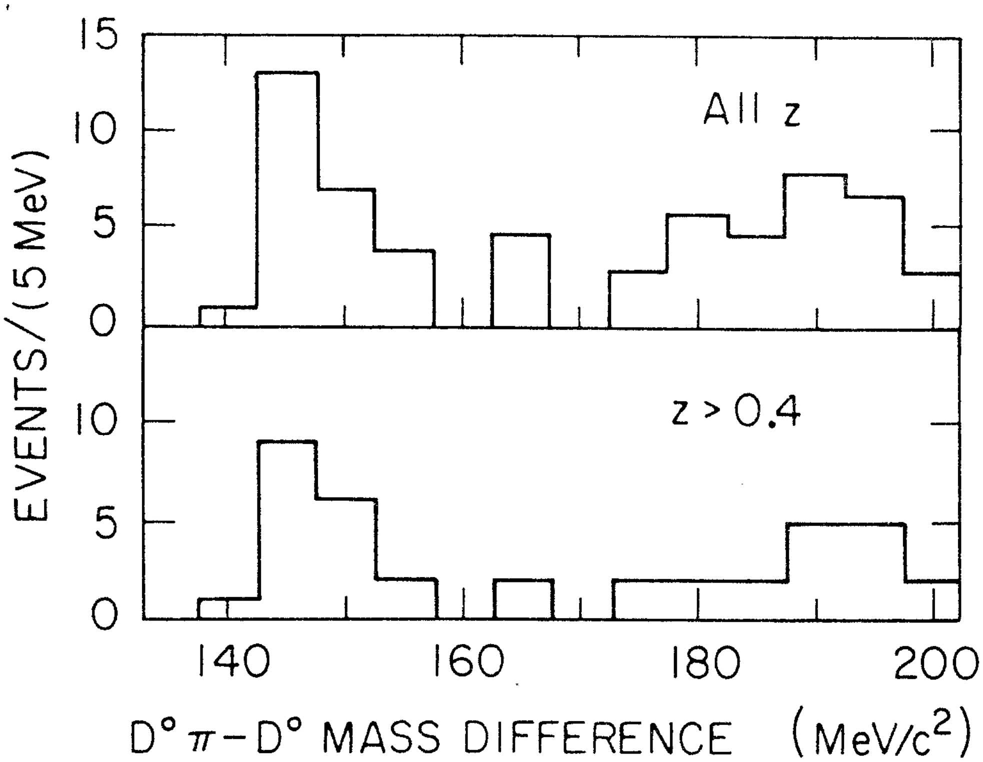

15
10
5
0
10
5
0
EVENTS/(5 MeV)
All z
z > 0.4
140
160
180
200
D° π − D° MASS DIFFERENCE (MeV/c²)

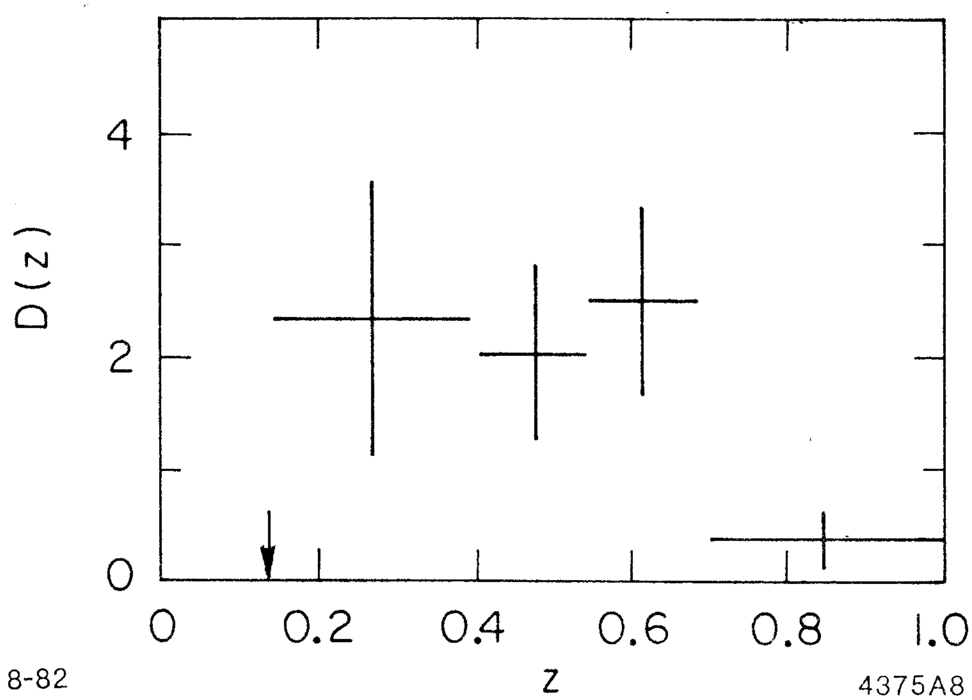

4
2
0
D(z)
0
0.2
0.4
0.6
0.8
1.0
z
8-82
4375A8

Fig. 6b

Fig. 7a

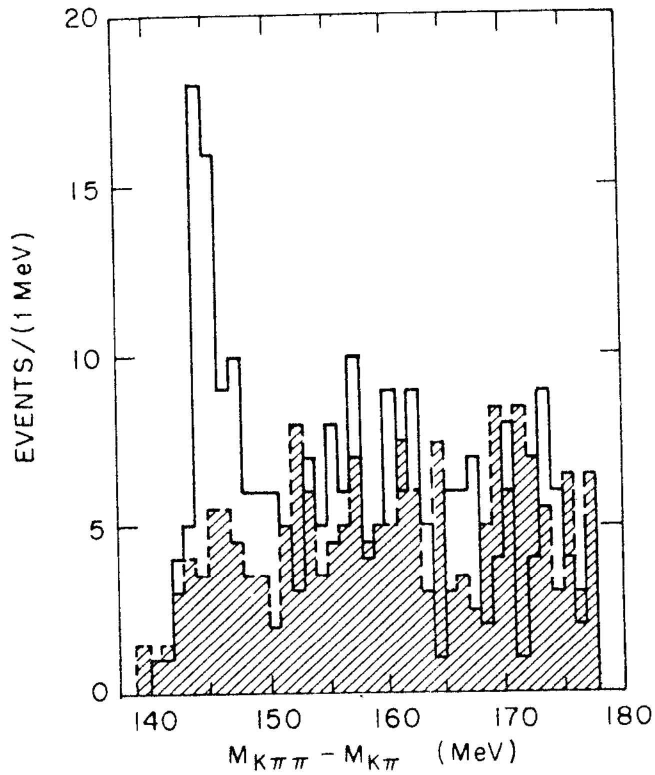

20
15
10
5
0
EVENTS/(1 MeV)
140
150
160
170
180
$M_{K\pi\pi} - M_{K\pi}$ (MeV)

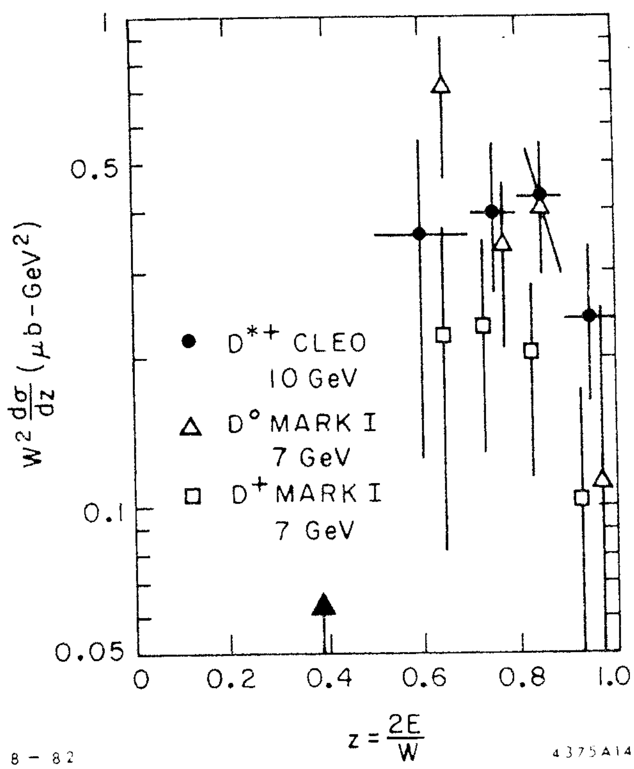

1
0.5
0.1
0.05
$W^2 \frac{d\sigma}{dz}$ (μb-GeV^2)
● D^{*+} CLEO 10 GeV
△ D° MARK I 7 GeV
□ D^{+} MARK I 7 GeV
0
0.2
0.4
0.6
0.8
1.0
$z = \frac{2E}{W}$
8 - 82
4375A14

Fig. 7b

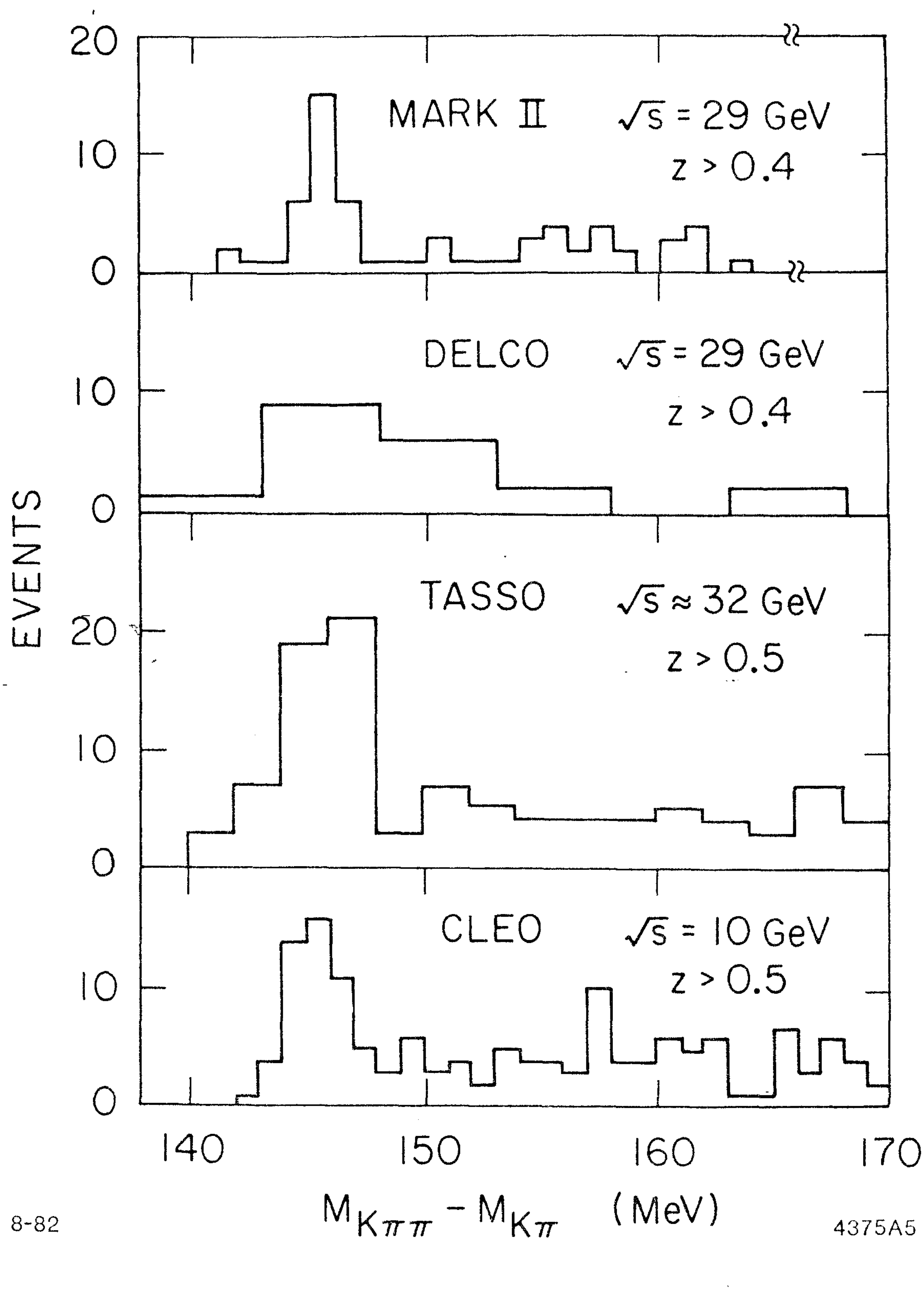
20
10
0
MARK II
√s = 29 GeV
z > 0.4
DELCO
√s = 29 GeV
z > 0.4
TASSO
√s ≈ 32 GeV
z > 0.5
CLEO
√s = 10 GeV
z > 0.5
EVENTS
140
150
160
170
M_Kππ - M_Kπ (MeV)
8-82
4375A5

Fig. 8

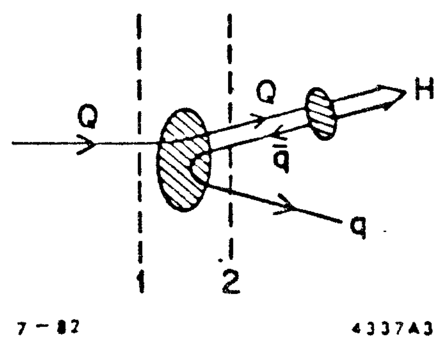

Fig. 9

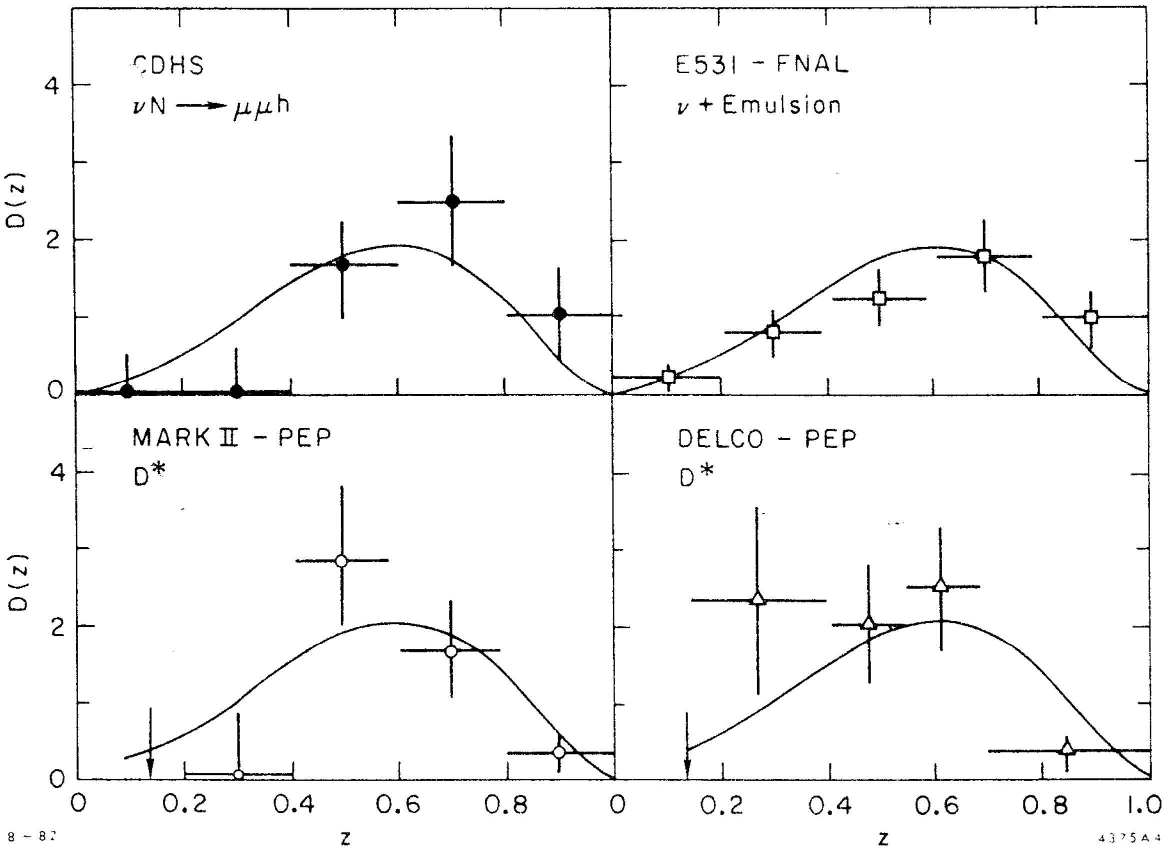
CDHS
νN ⟶ μμh
E531 - FNAL
ν + Emulsion
MARK II - PEP
D*
DELCO - PEP
D*
D(z)
D(z)
4
2
0
4
2
0
0
0.2
0.4
0.6
0.8
0
0.2
0.4
0.6
0.8
1.0
z
z
8 - 82
4375A4

Fig. 10

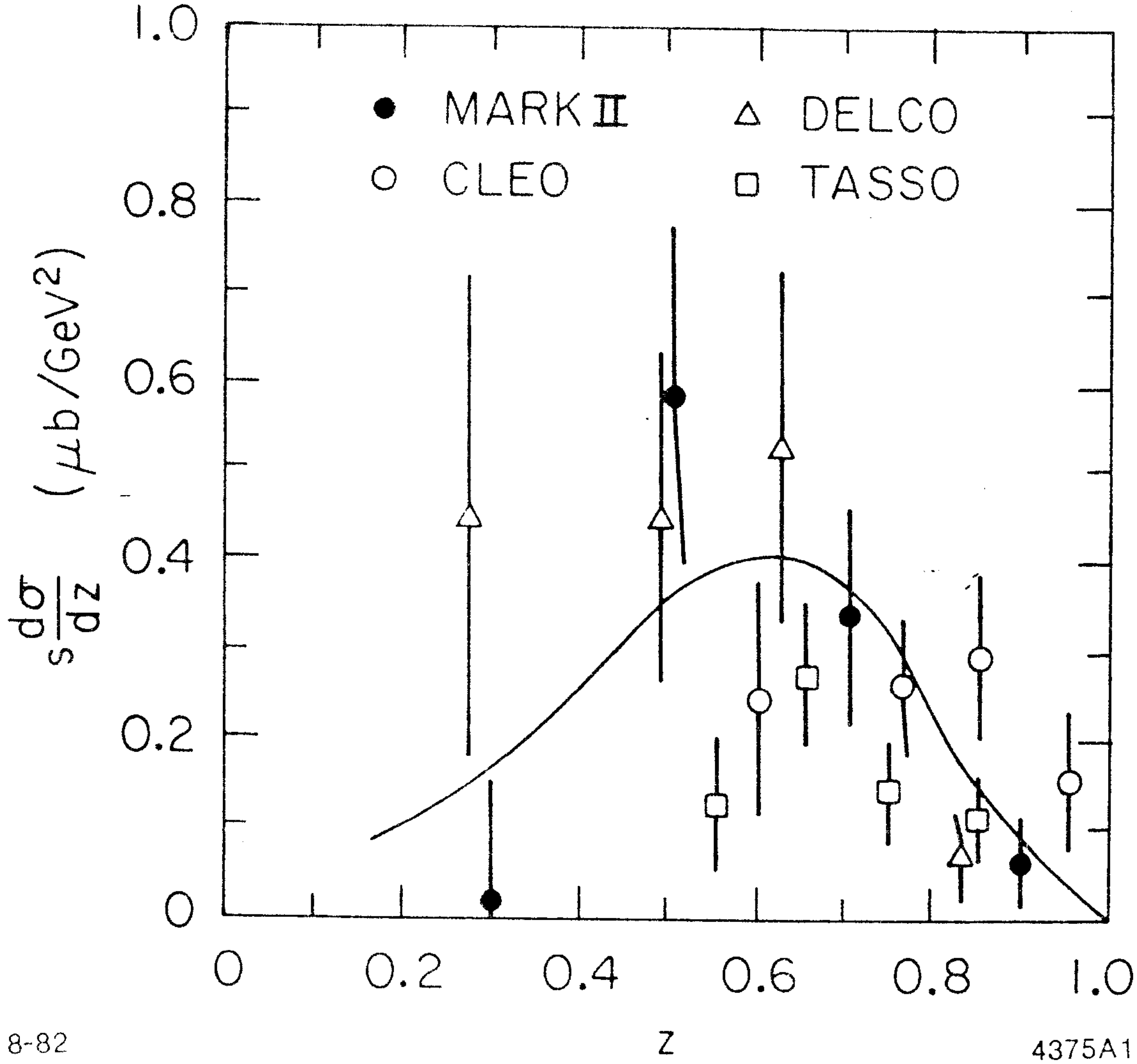

1.0
0.8
0.6
0.4
0.2
0
$s\frac{d\sigma}{dz}$ (μb/GeV^2)
MARK II
DELCO
CLEO
TASSO
0
0.2
0.4
0.6
0.8
1.0
8-82
Z
4375A1

Fig. 11

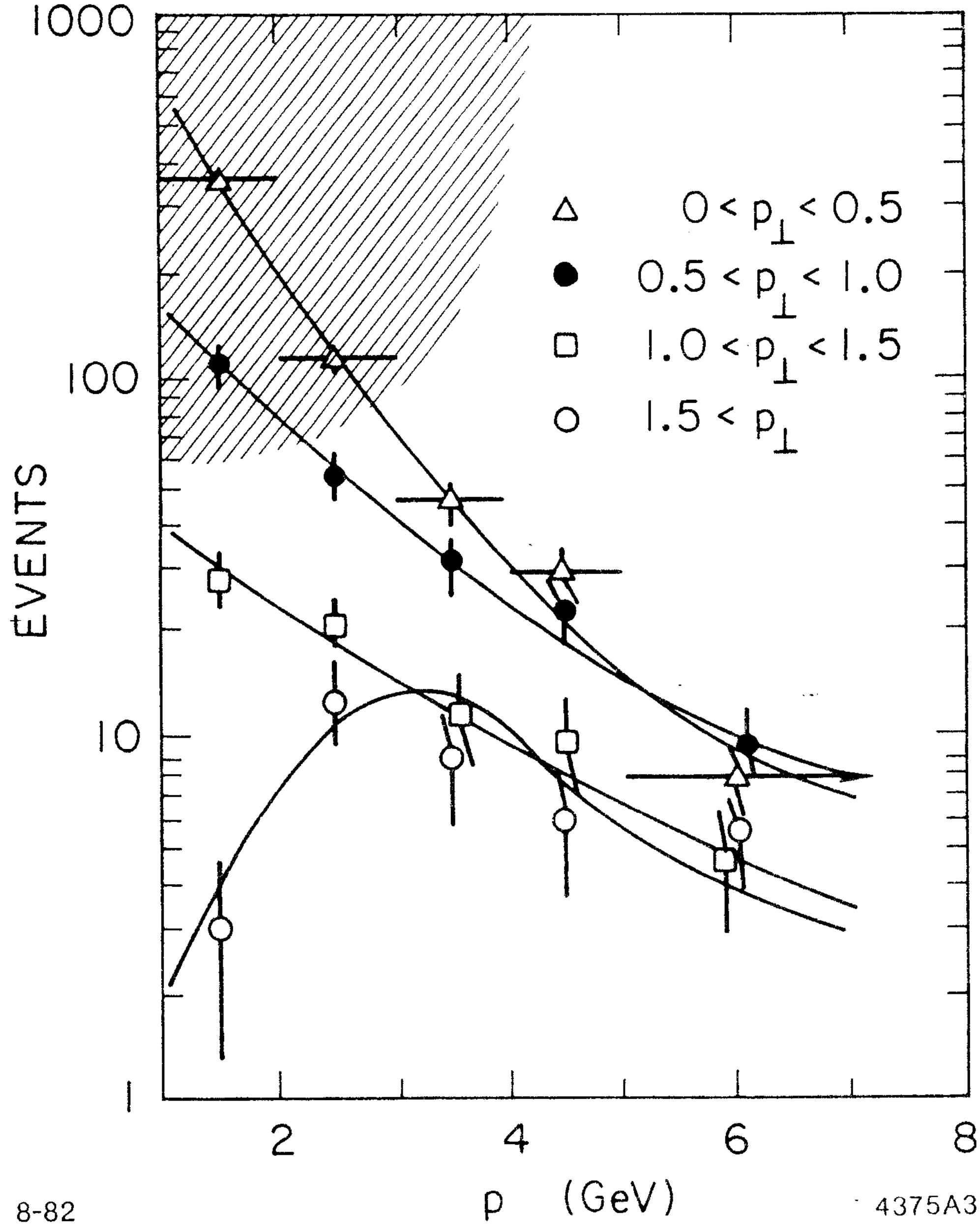
1000
100
10
1
EVENTS
0 < p⊥ < 0.5
0.5 < p⊥ < 1.0
1.0 < p⊥ < 1.5
1.5 < p⊥
2
4
6
8
p (GeV)
8-82
4375A3

Fig. 12

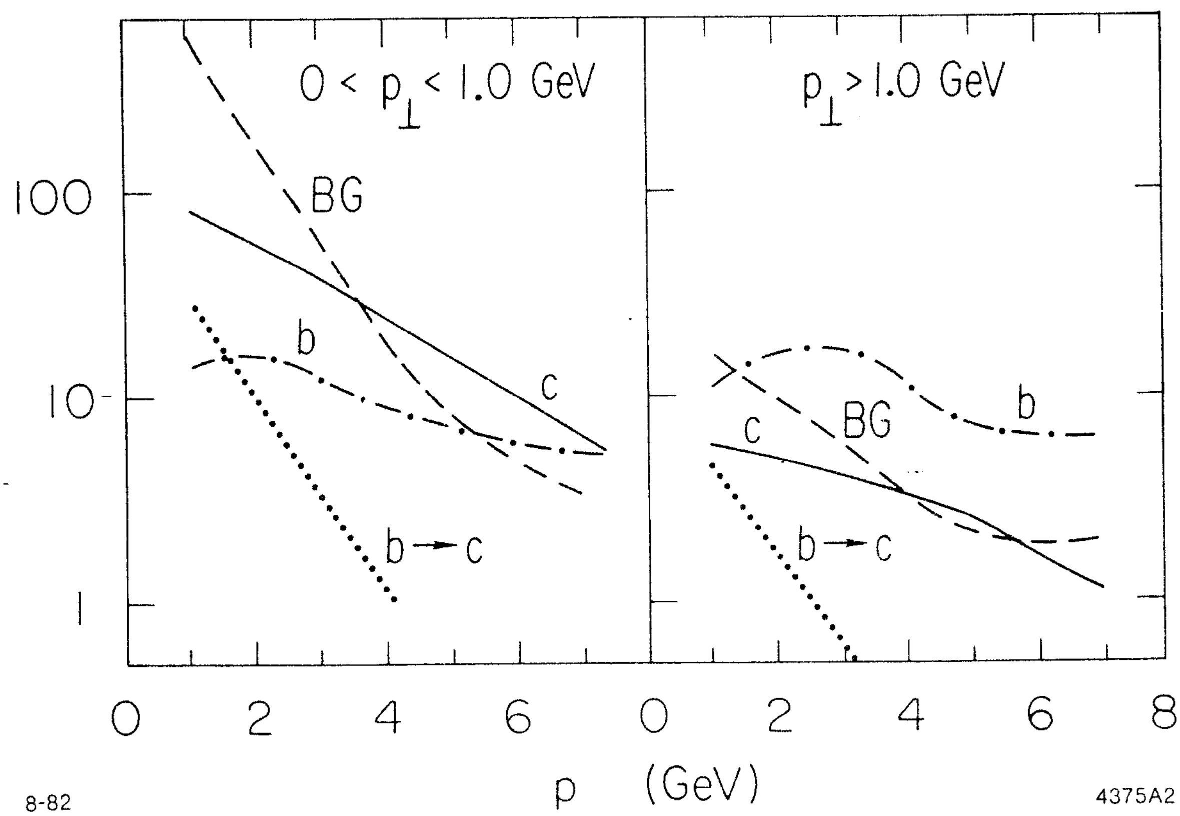

0 < $p_\perp$ < 1.0 GeV
$p_\perp$ > 1.0 GeV
100
10
1
BG
c
b
b → c
BG
c
b
b → c
0
2
4
6
0
2
4
6
8
p (GeV)
8-82
4375A2

Fig. 13

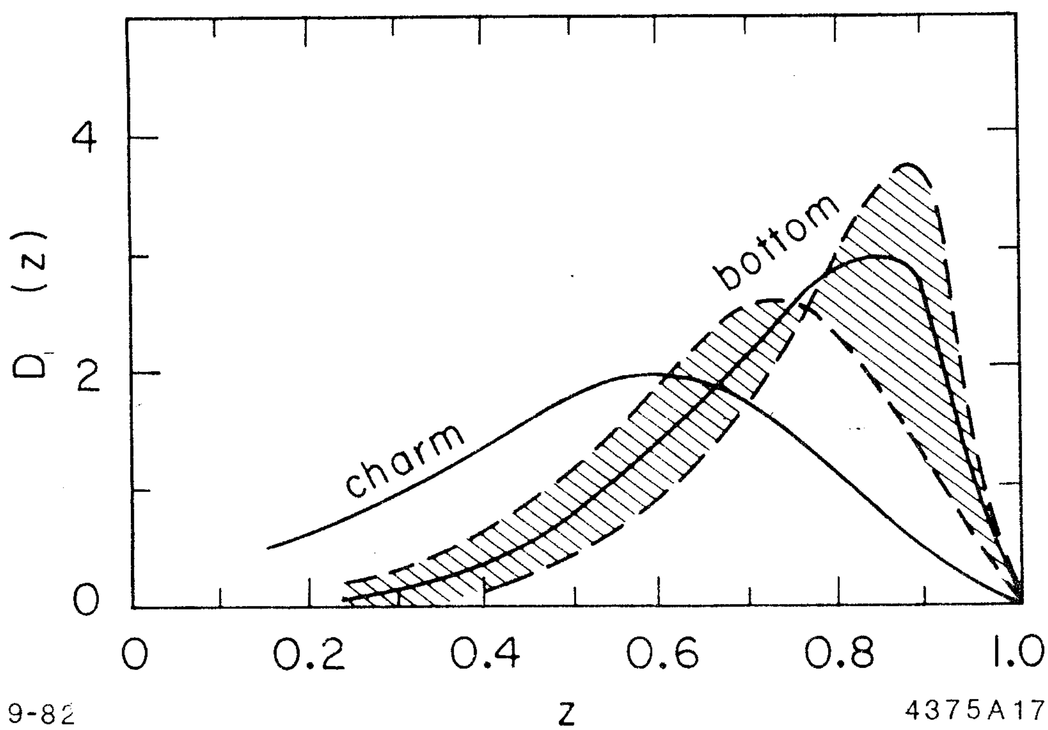

Fig. 14

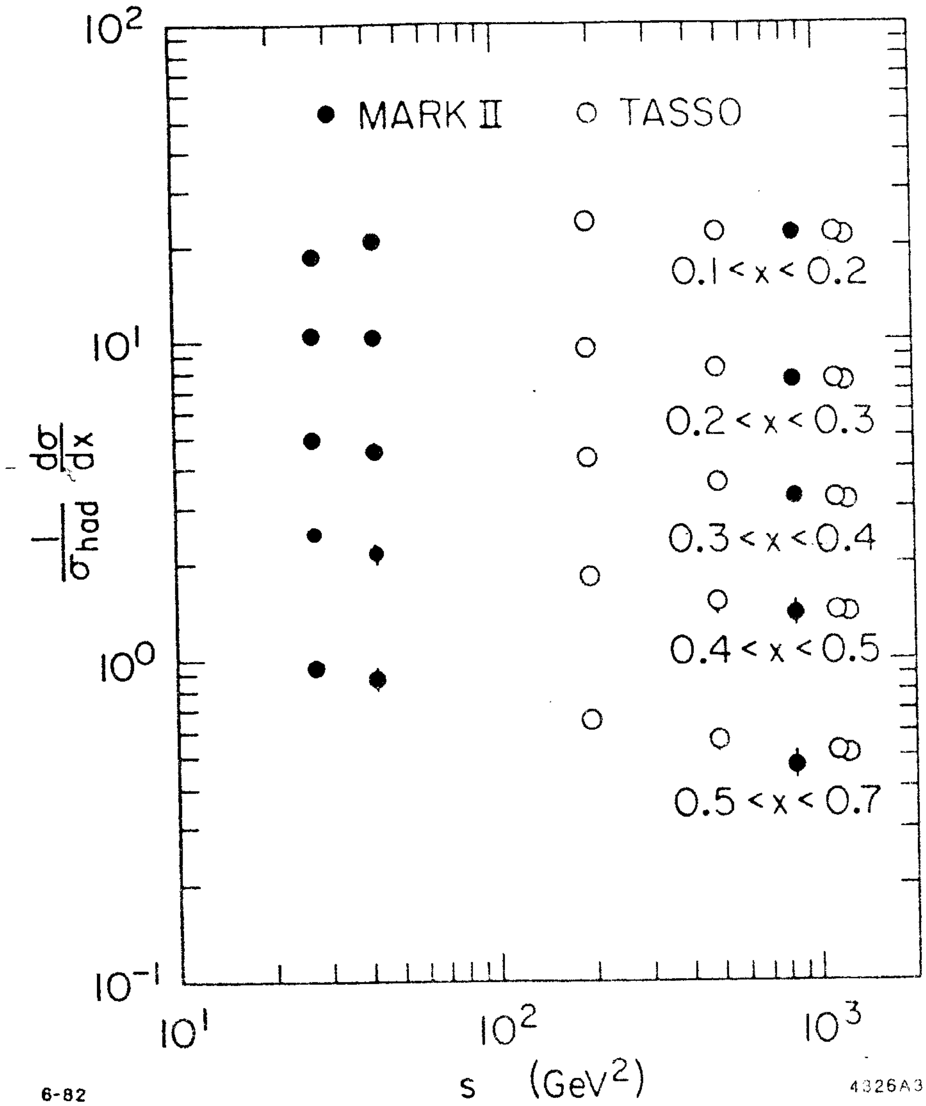

10^2
10^1
10^0
10^-1
● MARK II
○ TASSO
0.1 < x < 0.2
0.2 < x < 0.3
0.3 < x < 0.4
0.4 < x < 0.5
0.5 < x < 0.7
1/σ_had dσ/dx
10^1
10^2
10^3
s (GeV^2)
6-82
4326A3

Fig. 15

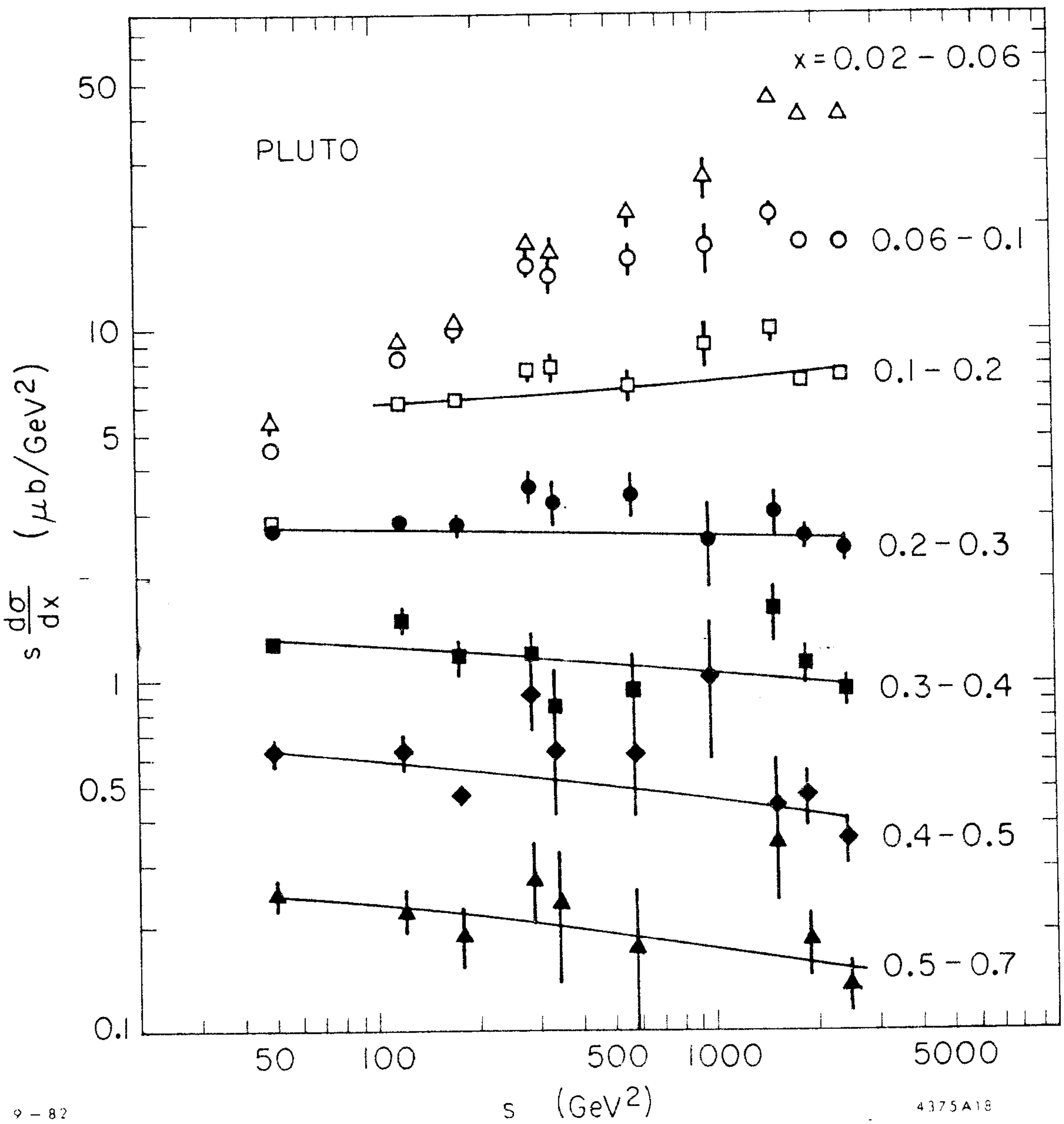

PLUTO
x = 0.02 - 0.06
0.06 - 0.1
0.1 - 0.2
0.2 - 0.3
0.3 - 0.4
0.4 - 0.5
0.5 - 0.7
s dσ/dx (μb/GeV²)
50
10
5
1
0.5
0.1
50
100
500
1000
5000
s (GeV²)
9 - 82
4375A18

Fig. 16

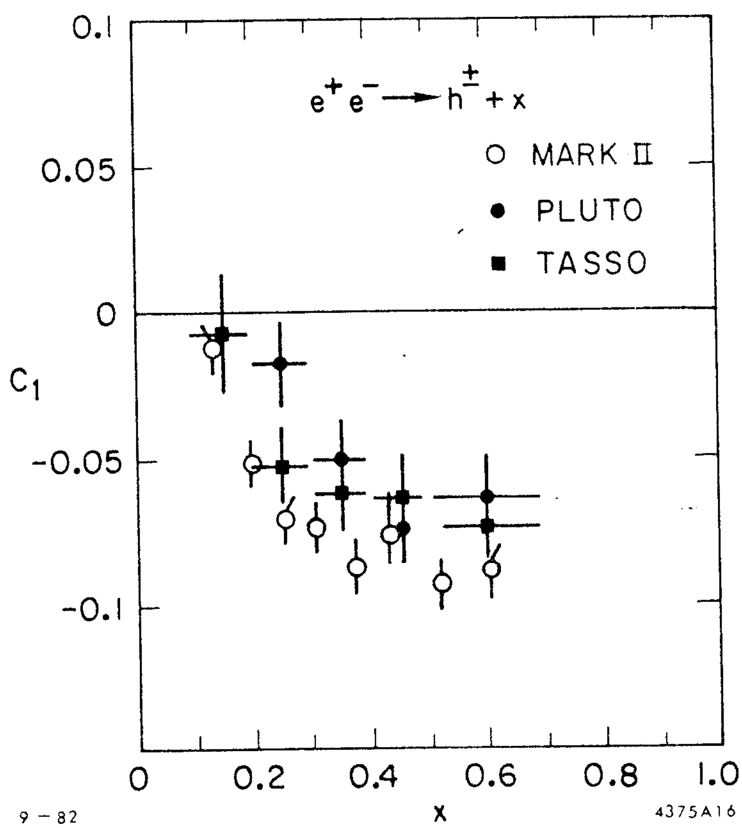

0.1
0.05
0
-0.05
-0.1
C_1
$e^+e^- \to h^\pm + x$
MARK II
PLUTO
TASSO
0
0.2
0.4
0.6
0.8
1.0
x
9 – 82
4375A16

Fig. 17

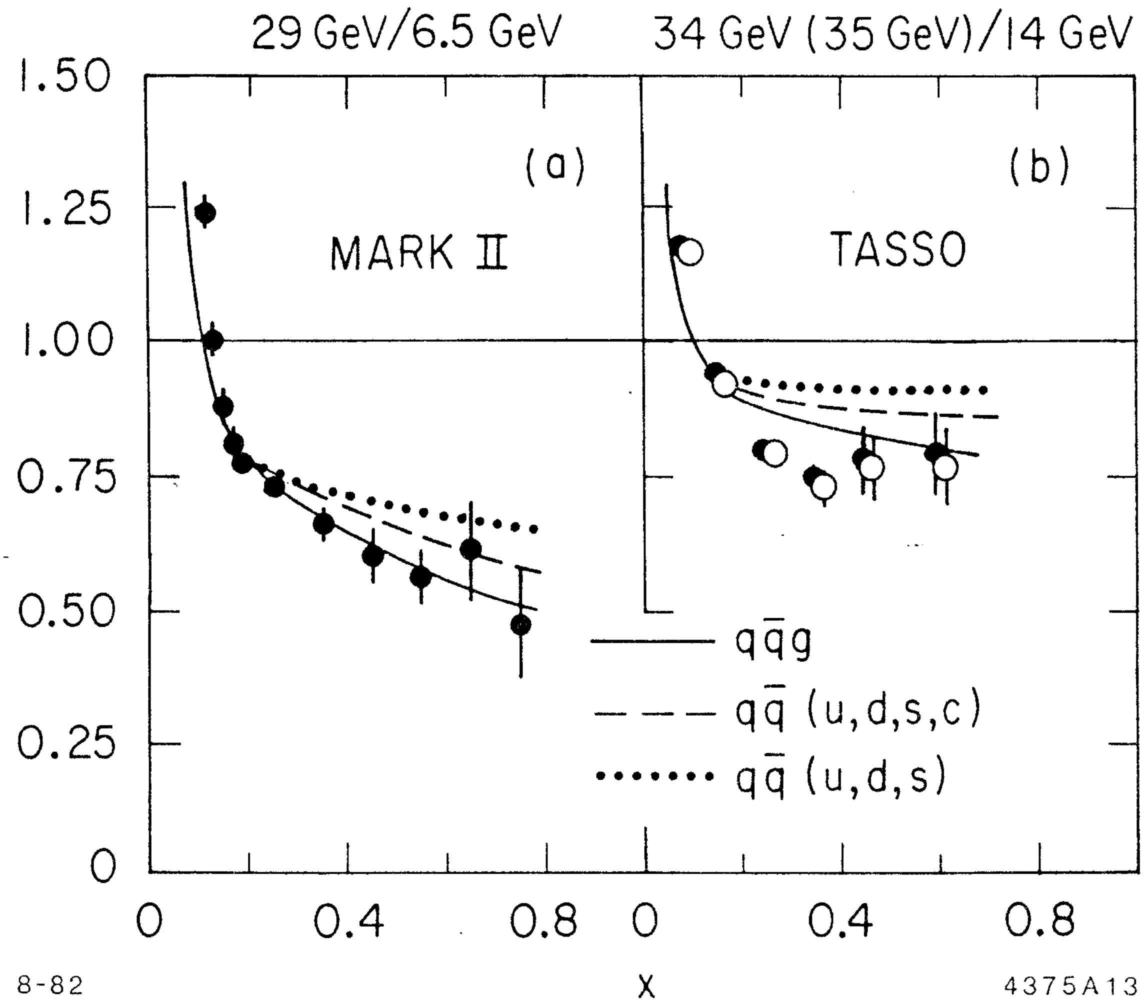

29 GeV/6.5 GeV
34 GeV (35 GeV)/14 GeV
1.50
1.25
1.00
0.75
0.50
0.25
0
(a)
MARK II
(b)
TASSO
$q\bar{q}g$
$q\bar{q}$ (u,d,s,c)
$q\bar{q}$ (u,d,s)
0
0.4
0.8
0
0.4
0.8
8-82
X
4375A13

Fig. 18